Journal of *Marine Science and Engineering*

MDPI

Article

Shallow-Water Submarine Landslide Susceptibility Map: The Example in a Sector of Capo d'Orlando Continental Margin (Southern Tyrrhenian Sea)

Elena Scacchia [1,*], Daniele Casalbore [2,3], Fabiano Gamberi [4], Daniele Spatola [2,*], Marco Bianchini [2,5] and Francesco Latino Chiocci [2,3]

1 ISPRA—Italian Institute for Environmental Protection and Research, 00144 Rome, Italy
2 Department of Earth Science, "La Sapienza" University, 00185 Rome, Italy
3 Istituto di Geologia Ambientale e Geoingegneria, National Research Council, 00185 Rome, Italy
4 ISMAR—Istituto di Scienze Marine, Sezione di Bologna, Consiglio Nazionale Delle Ricerche, 40129 Bologna, Italy
5 OGS—National Institute of Oceanography and Applied Geophysics, 34010 Trieste, Italy
* Correspondence: elena.scacchia@isprambiente.it (E.S.); daniele.spatola@uniroma1.it (D.S.)

Abstract

Active continental margins, generally characterized by narrow shelves incised by canyons, are pervasively shaped by submarine landslides that can occur near coastal areas. In this context, creating landslide susceptibility maps is the first step in landslide geohazard assessment. This paper focuses on shallow-water submarine landslides along the Capo d'Orlando continental margin and presents a related susceptibility map using the Weight of Evidence method. This method quantifies the strength of the association between a landslide inventory and predisposing factors. A geomorphological analysis of the continental shelf and upper slope yielded a landslide inventory of 450 initiation points, which were combined with five specifically selected preconditioning factors. The results revealed that the most favourable conditions for shallow-water landslides include slopes between 5° and 15°, proximity to faults (<1 km), proximity to river mouths (<2 km), the presence of consolidated lithologies and sandy terraces, and slopes facing NE and E. The landslide susceptibility map indicates that susceptible areas are in canyon heads and flanks, as well as in undisturbed slope portions near canyon heads where retrogressive landslides are likely. The model results are robust (AUC = 0.88), demonstrating that this method can be effectively applied in areas with limited geological data for preliminary susceptibility assessments.

Keywords: submarine landslides; slope instability; susceptibility map; weight of evidence; continental margin

Academic Editor: Chun-Feng Li

Received: 15 June 2025
Revised: 13 July 2025
Accepted: 14 July 2025
Published: 16 July 2025

Citation: Scacchia, E.; Casalbore, D.; Gamberi, F.; Spatola, D.; Bianchini, M.; Chiocci, F.L. Shallow-Water Submarine Landslide Susceptibility Map: The Example in a Sector of Capo d'Orlando Continental Margin (Southern Tyrrhenian Sea). *J. Mar. Sci. Eng.* **2025**, *13*, 1350. https://doi.org/10.3390/jmse13071350

1. Introduction

Submarine landslides are amongst the main marine geohazards [1–4]. They can result in landslide-generated tsunamis [5,6], in the destruction of seafloor infrastructures such as energy production infrastructures or cables [7,8], and the collapse of coastal areas into the sea [5,9]. Submarine landslides can produce large erosional features and are an important geological process for the transport of large amounts of sediment across the continental slope to the deep ocean [1,10–13]. Submarine landslides, which, in this paper, include the wide spectrum of submarine mass movements [10], are widespread processes at the shelf-edge and on the continental slope where steepness increases compared to the continental shelf.

Submarine landslides occurring in shallow-water settings, such as submarine canyons or shelf edges, are often distinguished from open-slope landslides based on their size and frequency [14–16]. Open-slope landslides, which originate from source areas on the continental slope and rise, are characterized by large volume displacements (ranging from millions of cubic meters to hundreds of cubic kilometres) [14], often occurring on gradients of less than 2° [3]. Large continental slope landslides are rare [17], but they have the potential to generate very damaging and far-traveling tsunamis [3]. In contrast, submarine canyons are complex and dynamic environments, characterized by steep slopes and typically affected by a greater number of landslides [18]. These failures usually mobilize relatively small volumes of sediment, ranging from hundreds of cubic meters to a few cubic kilometres [14]. Submarine landslides are the primary mechanism for canyon widening and headwall retrogression toward the coast [19–22]. Retrogressive failures at the canyon heads facilitate the transition from a slope-confined to a shelf-incised canyon [20,21]. The importance of retrogressive evolution caused by landslides is highlighted by the frequent occurrence of shelf-indenting canyons that seem to have no relation to the sediment supply systems [23,24]. Moreover, despite the limited volume of the failed mass, landslides occurring in submarine canyons close to the coastline can pose significant risks to coastal areas and infrastructure, as they have been shown to trigger tsunamis [5,9].

The recurrence of landslides in submarine canyons, which in the Italian peninsula can be very close to highly densely populated coastal areas, underlines the importance of developing landslide susceptibility maps in shallow-water sectors. Susceptibility analysis identifies where the environmental conditions make the seafloor prone to the occurrence of landslides and represents the first step in natural risk assessment. However, despite its importance, a search on Scopus for "submarine landslide susceptibility" yields only 21 papers worldwide, which all strictly related to the issue and are mainly based on the analysis of open-slope landslides. Therefore, it emerges that the scientific literature on landslide susceptibility maps for the marine environment is not as extensive as that related to the subaerial counterpart and does not sufficiently address landslides occurring in shallow-water sectors. To evaluate areas susceptible to submarine landslides, different statistical methods have been used to assess the correlation between preconditioning factors and landslides [25–28].

Preconditioning factors are long-lasting factors that influence slope stability but, unlike triggering factors, do not cause the margin to move from its stable or marginally stable state [29]. The most cited preconditioning factors are slope oversteepening, the presence of weak layers, high sediment rates, fluid charging, earthquakes, wave action, and volcanic activity [1,3,11–13]. Most of the existing studies on preconditioning factors are based on landslides occurring in open-slope settings and therefore may not fully capture the different geological and oceanographic conditions active in shallow-water environments. Considering these critical issues, we analyzed the morphological expression of submarine landslides in the shallow-water sector (e.g., continental shelf and the upper slope sectors until 300 m of depth) of the Capo d'Orlando continental margin, northern Sicily, to answer the following research questions:

(i). Which geological factors that can be extensively mapped have a preconditioning value for the formation of shallow-water landslides in the study area?
(ii). What are the most favourable preconditioning conditions to promote shallow-water landslides?
(iii). Which seafloor sectors are more susceptible to instability processes?

2. Geological, Climatic and Oceanographic Setting

The Capo d'Orlando continental margin lies off the north-eastern sector of Sicily (Figure 1). The current geological-structural setting of the Capo d'Orlando continental margin has been controlled by the geodynamic evolution of the central Mediterranean, with reference to the collisional processes between the African and Eurasian plates resulting in the Sicilian fold and thrust belt [30]. In the northern Sicilian area, a post-orogenic extensional tectonic regime was established through the formation of a series of extensional faults that caused the fragmentation of the orogenic chain into structural highs and troughs where marine sedimentary basins formed, e.g., Capo d'Orlando Basin (Figure 1a) [31–34].

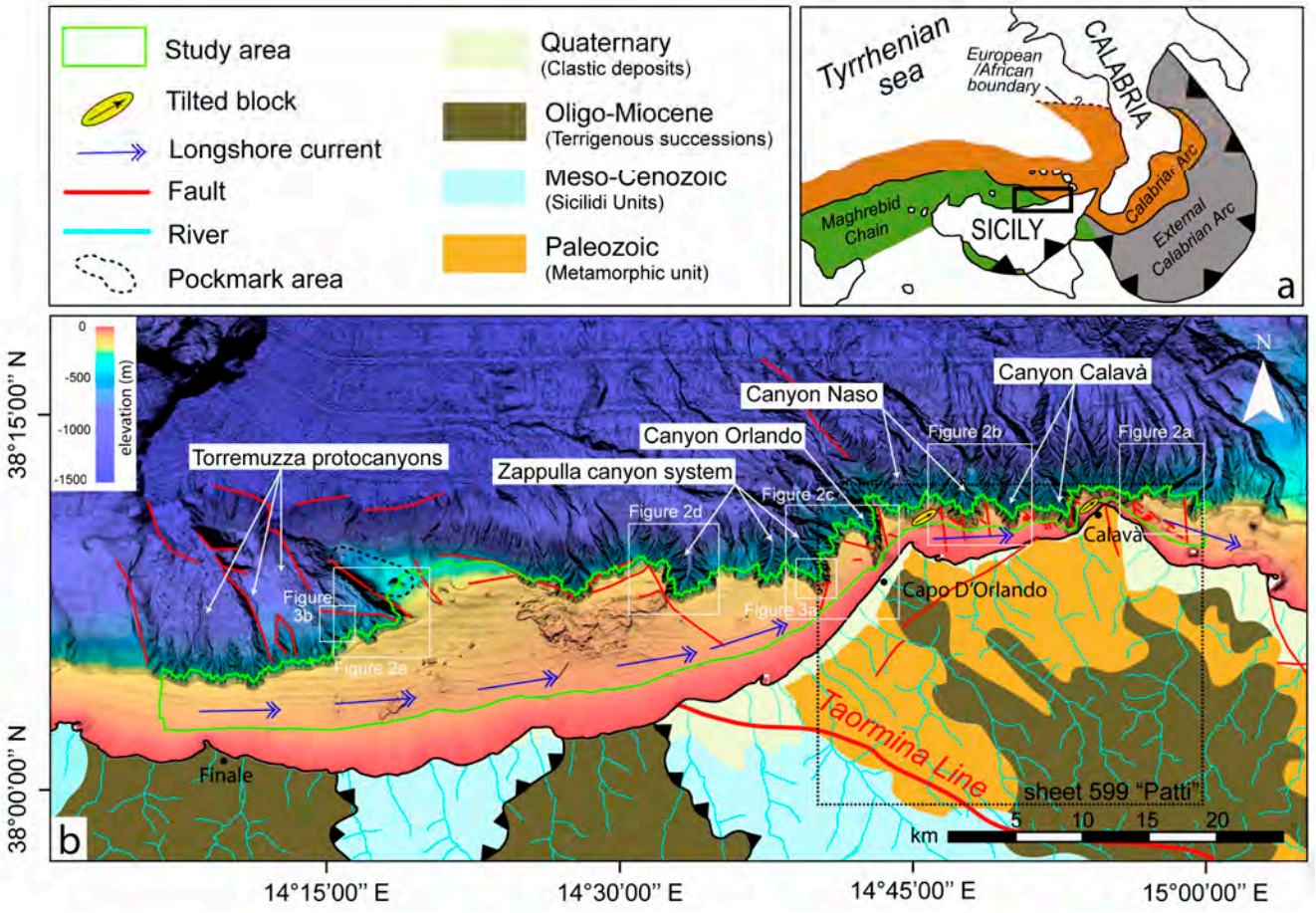

Figure 1. (**a**) Schematic structural map of the central Mediterranean (modified from Catalano et al., 2013 [35]). The inset shows the location of the study area. (**b**) Shaded relief map of the Capo d'Orlando continental margin and the study area highlighted by the green polygon. The names of the principal towns and canyon systems are reported, as well as the faults dissecting the continental margin, the location of tilted blocks, pockmarks, and the direction of longshore currents. The geological map of the emerged portion to the south of the study area is modified from [35], and faults are extrapolated from the METIQ project.

The study area pertains to the east of the Sicilian sector of the Calabrian arc and is separated by the Taormina Line from the Maghrebid chain to the west (Figure 1). Onland, Paleozoic metamorphic terrains outcrop to the east, overlaid by an Oligocene-Miocene terrigenous cover consisting of flyschoid formations that, in the western sector, are overthrusted by Meso-Cenozoic Sicilidi Units (Figure 1b) [30]. In the eastern submarine portion of the study area (Figure 1b), Upper Pliocene—Upper Pleistocene Noemi Unit outcrops in coincidence with canyons; it comprises hemipelagic and turbiditic deposits covered, in the continental shelf, by late Quaternary depositional sequence [35].

Very recent extensional faults (0.5 Ma-recent) are oriented in a NE–SW and NW–SE and E–W direction (Figure 1b) [33,36], separating the basin characterized by a strong and active subsidence from the surrounding coastal areas affected by high uplift rates [37,38]. In the eastern sector, coastal uplift values reach 1 mm/yr and decrease to the west reaching maximum values of 0.35 mm/yr in the Finale area [37–40]. Tilted surfaces recognized on the outer continental shelf between Capo d'Orlando and Capo Calavà are the morphological expression of the recent activity of extensional faults (Figure 1b) [40].

From a meteo-marine point of view, the northern coast of Sicily is affected by sporadic winter storms and by seasonal wind-driven currents [41,42]. In the study area, sediments generally reach the coastal region during the winter storm season through intermittent river courses named "Fiumare". Longshore currents, moving parallel to the coast according to the wind direction, are one of the principal mechanisms driving sediment transportation and deposition in the study area and have an overall west–east direction (Figure 1b) [24,43,44].

3. Geomorphology of the Capo d'Orlando Continental Margin

The study area (415 Km^2, Figure 1b) encompasses most of the Capo d'Orlando continental shelf and upper slope. The study area has a width, from S to N, of 11 Km at its most and 1 km at its minimum and spans the bathymetric range between 12 m and 300 m (Figure 1b). In the eastern sector, the continental shelf is narrow and the shelf edge is incised by numerous canyons with a NW–SE direction (Figure 1b). From east to west, the main canyons are Calavà (also called "Gioiosa Marea"), Naso, Orlando, and Zappulla (Figure 1b).

- Calavà canyon: Calavà canyon-head is a few tens of meters from the coast at 5 m of depth (Figure 2a) and is directly connected to a river [24,45]. In the continental shelf surrounding the Calavà canyon continuous steps created by the foresets of submarine depositional terraces (i.e., sand-rich prograding wedges) [46] are recognized at different depths, i.e., 30 and 50 m, and their lateral continuity is occasionally interrupted by canyon heads (Figure 2a,b) [47].
- Orlando canyon: Orlando canyon has its head at 30 m of depth, about 500 m from the coast and is directly connected to a river (Figure 2c). The Orlando canyon has a mixed alimentation, it is fed by river inputs and littoral drift flowing from W to E and carrying sediment-laden flows into the canyon [24].
- Naso Canyon: The canyon head is located at 2 km from the homonymous river mouth at a depth of 30 m, it is suggested to have its morphology controlled by a fault [24].
- Zappulla canyons: Three canyons make up the Zappulla canyon system (Figure 1). The easternmost Zappulla canyon is located 2 km from the coast at—75 m in front of a river mouth delivering sediment until the canyon head, as proved by the presence of gullies on the continental shelf (Figure 2c). The westernmost Zappulla canyon is located where the continental shelf is 10 km wide. Here, the canyon head indents the continental shelf at 100 m depth in front of a large outcropping bedrock (Figure 2d). In the area behind the canyon head, transgressive sandy deposits corresponding to deltas, bars, tombolos, and spits have been recognized (Figure 2d) [45]. To the west with respect to the Zappulla canyon, a triangular-shaped block is characterized by the presence of pockmarks aligned in a NW–SE direction (Figure 1b).

In the western extremity of the Capo d'Orlando continental margin, the shelf decreases to 4 km due to landslide retrogression at the head of incipient Torremuzza proto-canyons with a shelf-edge at 150 m depth. Landslide scars are pervasive in the study area, characterizing both the canyons and open slope portions (Figure 3). Generally, most of the landslides occurring in canyons have coalescent scars and do not exhibit a detectable deposit in the present-day bathymetry (Figure 3a). The distribution and morphology of landslides in the

Capo d'Orlando canyons are similar to those classified as 'disintegrative slides' observed along canyons in the Calabro–Tyrrhenian continental margin [48]. Landslides occurring on open slopes are larger than those occurring in canyons (note the difference between scar lengths in Figure 3) and are characterized by steep headwall slopes and the permanence at the base of the headwall of part of the deposits (Figure 3b).

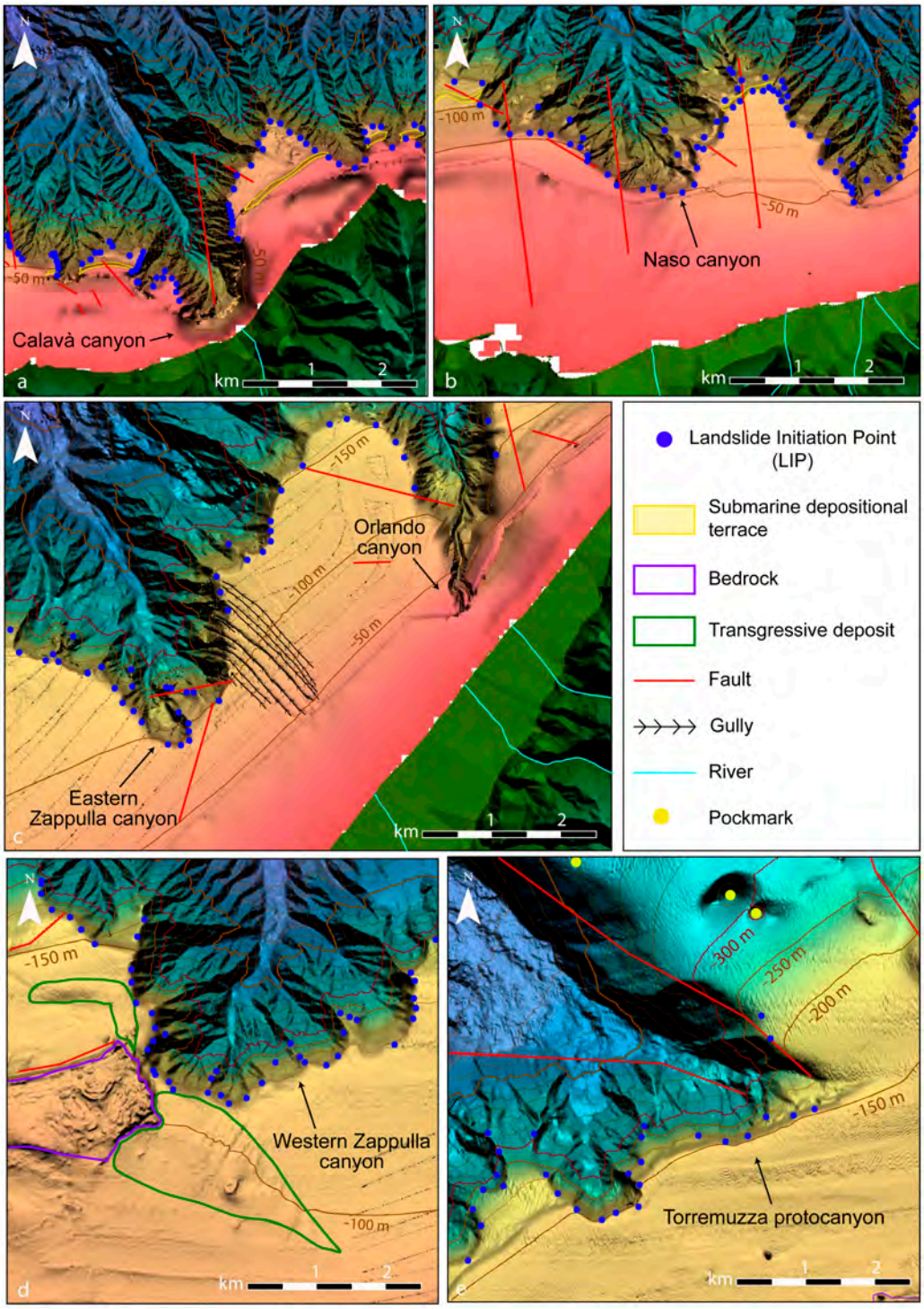

Figure 2. Zoom of portions of the study area (insets (**a**–**e**)) characterized by the presence of canyons and gullies close to river mouths. Faults dissecting the continental shelf and upper continental slope are traced as the morpho-lithological elements (e.g., bedrock outcrop, submarine depositional terraces foresets, and transgressive deposits). Contours are marked every 50 m, and the study area is limited by 300 m depth contour.

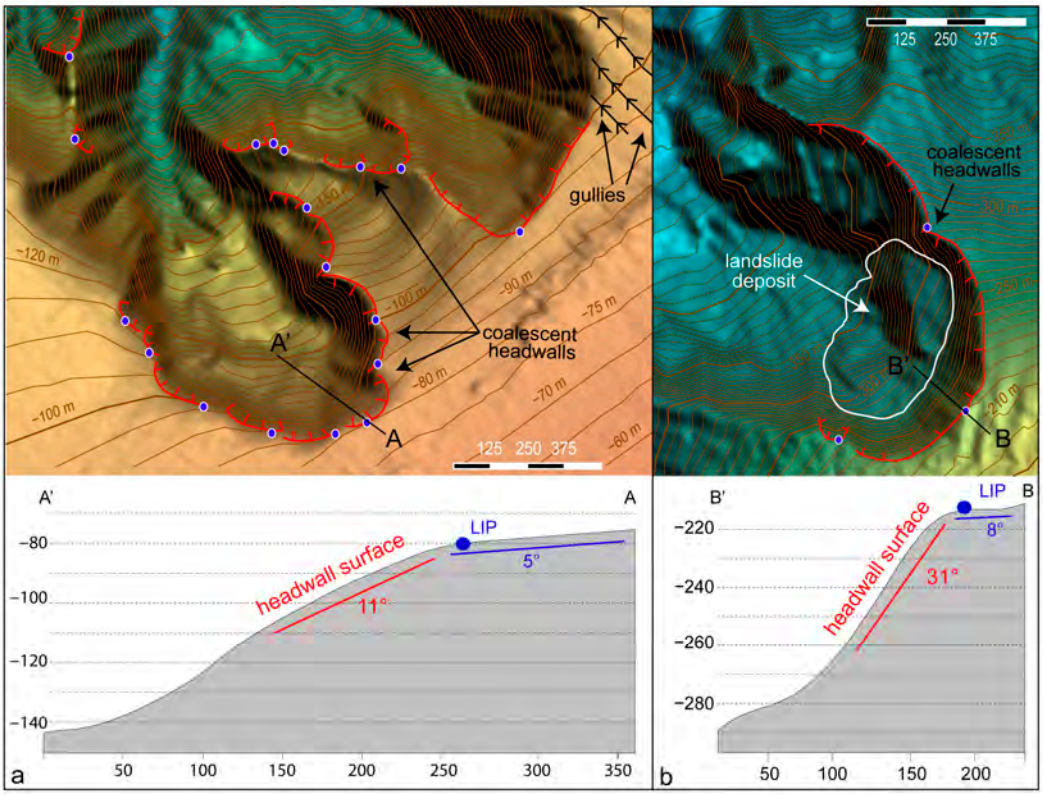

Figure 3. Landslide elements mapped in the study area. Note the presence of coalescent scars and the location of the LIPs (blue point) used to approximate the slope morphology before the instability process. (**a**) Landslides at canyon head and flank, and a topographic profile crossing one of the headwalls. (**b**) Open-slope landslides and a topographic profile crossing one of the headwalls.

4. Materials and Methods

4.1. Geophysical and Landslides Dataset

The geomorphological framework of the study area is based on a Digital Terrain Model (DTM) with 10 m resolution gridded using bathymetric data acquired within MAGIC project (Marine Geohazards along the Italian Coasts) on board the R/V Mariagrazia with a Reson 7111 working at a frequency of 100 kHz (Figures 1 and 2).

Landslide headwalls have been mapped as linear elements from which the highest points along the headwall have been extracted and associated with the Landslide Initiation Point (LIP, blue points in Figure 3). LIPs are commonly used in subaerial landslide susceptibility analysis to approximate the slope condition before the instability process [49–51]. Due to the extreme tendency to have landslide coalescence at the canyon heads, we mapped single headwalls based on their semicircular shape with respect to the nearby coalescing features. Specifically, whenever a noticeable change in the curvature direction of the headwall occurred, we interpreted it as the onset of a different landslide crown and mapped it as a separate feature. Scarps formed by erosive processes due to turbidity currents and hyperpycnal flows able to rework the seafloor morphology, recognized by the presence of gullies, have been excluded from the model. According to this approach, 450 LIPs have been mapped (Figure 2), and, together with the preconditioning controlling factors, were used to capture potentially unstable slope conditions.

4.2. Preconditioning Factors

In this work, a set of 5 raster maps with a 10 m-grid cell has been used to consider the following preconditioning factors: slope, aspect, simplified lithology, distance from river mouths, and distance from faults.

- Slope, surface steepness measured in degrees, is considered the most important factor affecting slope stability [52,53], since the driving force of mass movement increases with increasing slope. According to the literature, slope classes are commonly divided at intervals of 5° [52]; consequently our slope map is divided into ten classes from <5° to >45° (Figure 4a).

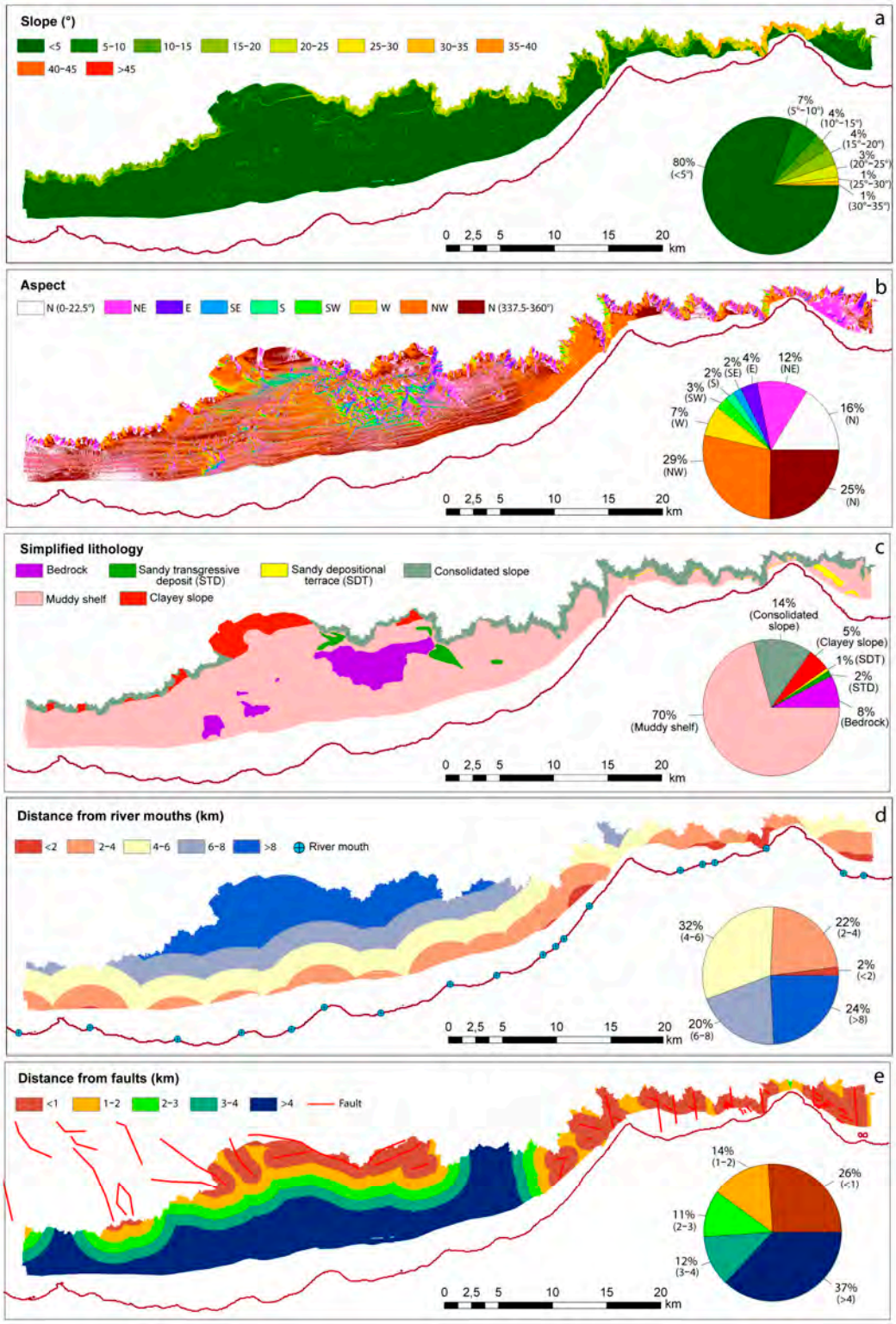

Figure 4. Preconditioning factors of shallow-water landslides in the study area. Slope (**a**), aspect (**b**), simplified lithology (**c**), distance from river mouths (**d**), and distance from faults (**e**). The pie charts illustrate the areal percentage of each factor class.

- Aspect indicates the compass direction that a slope faces, corresponding to the direction of the steepest slope at each point on the terrain surface [54]. In submarine environments, the aspect map can emphasize morphological differences controlled by the action of oriented water masses (e.g., wave action, longshore currents) that control the accumulation or the transport of sediment on the continental shelf and shelf-indented canyons. For this reason, the aspect map is considered in the analysis and is divided into 9 classes representing the slope directions generally used for landslide analysis [54] (Figure 4b).
- The Simplified lithological map has been produced in the study area assigned to the different depositional environments (i.e., continental shelf, slope); it deposits (i.e., depositional terraces, transgressive deposits) the lithology conventionally associated with them. This approach resulted in the recognition of a clayey slope, Consolidated slope, muddy shelf, sandy depositional terrace, sandy transgressive deposits, and bedrock (Figure 4c). Transgressive deposits have been extracted from [45], while the foresets' extension of depositional terraces and outcropping bedrock from the MAGIC project [47]. The distinction of a consolidated slope relies on the presence of canyons deeply incised on the slope eroding and exposing older and presumably more consolidated sedimentary sequences (i.e., Noemi Unit) compared to late Quaternary depositional sequences characterizing the continental shelf.
- *Distance from river mouths* is considered a possible preconditioning factor for shallow-water landslides. Fiumare, the typical rivers of the study area, have a torrential regime and may experience flash flood events with high sediment/water ratio (>5–10%), which can exert important shear stress on the seafloor or rapidly deposit their sediment load increasing pore water pressure [55]. For this reason, the river-mouth distance map was extracted based on the Italian drainage network and divided into five classes with a 2 km interval (Figure 4d).
- *Distance from faults* is used to evaluate the importance of oversteepening of morphological fault steps able to form potential sliding surfaces, enabling detachments and downslope movements of sediment volumes. Faulting within the sedimentary column can also generate deformations in unconsolidated sediments and produce loose cataclastic debris within hard bedrocks forming weak layers that reduce overall slope stability. In our analysis, faults have been extrapolated from METIQ sheet 5 [56], sheet 599 "Patti" [35] and, in the western part of the Capo d'Orlando continental margin, through the interpretation of the available seismic profiles [57] (Figure 1b). The distances from the faults have been divided into five classes with 1 km intervals (Figure 4e).

4.3. Weight of Evidence (WoE) Method

Susceptibility for shallow-water submarine landslides was carried out applying the WoE method through the specialized "graphical user interface" (GUI) for ground instability susceptibility analysis developed in MATLAB R2024a. WoE is a statistical method commonly employed in predictive modelling and risk assessment; it quantifies the strength of association between predictor variables (preconditioning factors) and the occurrence of submarine landslide (LIPs). This model is based on the determination of positive (W+, 1) and negative weights (W−, 2) for each class of preconditioning factors based on the presence or absence of landslides within the area as indicated by the following equation [58]:

$$W+ = \ln\left(\frac{\frac{A1}{A1 + A2}}{\frac{A3}{A3 + A4}}\right), \quad (1)$$

$$W- = \ln\left(\frac{\frac{A2}{A1 + A2}}{\frac{A4}{A3 + A4}}\right), \quad (2)$$

where A1 is the number of LIPs in each factor class, A2 is the number of LIPs absent in the given factor class, A3 is the number of the cells in the given factor class in which no LIPs are present, and A4 is the number of cells in which neither LIPs nor the given factor class is present. The difference between W+ and W− is the contrast index (C). The magnitude of C reflects the strength of the predictor's impact, highlighting the relevance of each factor in contributing to the event's occurrence. The overall landslide susceptibility (LS) for each cell is computed by summing the contrast values of each factor:

$$LS = \sum_{i=1}^{n} Ci, j \quad (3)$$

where Ci,j is the contrast value for the class j of factor i and n is the total number of factors. The GUI trains and validates the model with a certain percentage of the LIPs. In our study, 70% of the targets were used to train, and the remaining 30% to test the model as commonly adopted in susceptibility analysis performed through WoE [59,60]. The susceptibility map provided by the GUI is normalized into a 0–1 range that indicates the probability of instability in that pixel. A receiver operating characteristic (ROC) curve, which plots the true positive rate against the false positive rate, is calculated for the training, test, and entire area dataset. The area under the ROC curve (AUC) quantifies the model's potential discriminating power; values above 0.7 are generally considered indicative of acceptable predictive performance.

5. Results

5.1. Preconditioning Factor Classes Distribution

Figure 4a shows that 80% of the study, mostly localized in the continental shelf, shows gentle slope gradients (<5°). Slopes between 5° and 35° cover 18% of the study area (Figure 4a) and are mainly measured along canyon systems in the consolidated slope (17%), with smaller portions along bedrock outcrop edges (8%) and foresets of submarine terraces (1%) (Figure 4c). The highest slope values (>35°) are localized along the eastern sector on the sidewalls of the Calavà and Naso canyon and are less than 1% (Figure 4a). The slope is prevalently exposed to the north (41%), northwest (28%), and northeast (16%) (Figure 4b). Seafloor areas facing west represent 7% of the total, with even less exposure in the other directions (Figure 4b). Nineteen river mouths, especially to the west and to the east of the study area, are proximal to the shelf edge (Figure 1b). Nevertheless, the sectors localized at less than 2 km from a river mouth represent a small part of the study area (2%, Figure 4d), the 22% is 2–4 km away from it, while the rest is located more than 4 km away (Figure 4d). The study area contains numerous mapped faults mainly localized on the eastern and central sectors (Figure 1b). In fact, 26% of the area is located within 1 km from faults and 14% from 1 to 2 km of distance, while the highest percentage is found in areas more than 4 km away from the faults (about 37%, Figure 4e).

5.2. Contrast Values of Preconditioning Factors Classes

The variable weights of the different preconditioning factors in the instability process can be understood by examining the bar plots in Figure 5 and are reported in Table 1. These plots show the contrast for each class of preconditioning factors across the LIPs. Regarding the slope, the highest positive incidence for landslides occurs in the range from 5 to 15° (C = 2.30–2.31). Negative values of contrast are recorded in slopes less steep than 5° and steeper than 25° (e.g., C = −3.51 for <5°). The aspect contrast indexes are positive for slopes oriented towards NE (C = 0.88), E (C = 0.36), and N (0–22.5°, C = 0.28), whereas the SE (C = −1.22), NW (C = −0.61) and N (337.5–360°, C = −0.61) aspects exhibit negative correlations. According to the simplified lithology parameter, landslides positively correlate with the presence of sandy depositional terraces (C = 1.20) and consolidated slopes (C = 1.17). In contrast, shallow-water landslides negatively correlate with clayey slope (C = −0.23) and muddy shelf class (C = −0.54). The distance from the river shows that a strongly positive incidence characterizes the distance from river mouths <2 km (C = 1.71), followed by 2–4 km class (C = 0.54) and the correlation decreases at increasing distances. A similar behaviour characterizes the distance from fault parameters, which positively correlates with landslides when they are at <1 km of distance (C = 1.77) and 1–2 km of distance (C = 0.27), while at increasing distance the correlation is negative. In conclusion, according to the contrast index values, the most relevant factors for landslide occurrence are slope, followed by distance from faults and distance from river mouths, simplified lithology, and aspect (Figure 5).

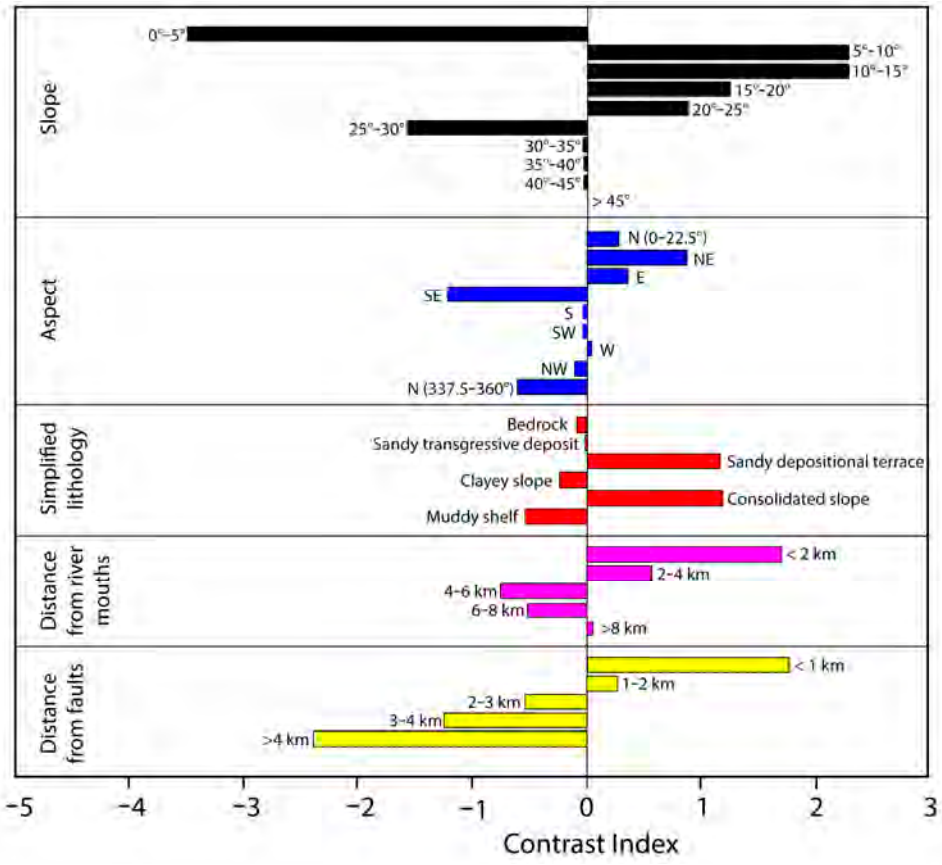

Figure 5. Bar plots showing the contrast index for each class of the preconditioning factors related to LIPs. Contrast index values are reported in Table 1.

Table 1. Spatial relationship between each class of preconditioning factors and landslides extracted using the WoE method.

Variable (Unit)	Class	Description/Numerical Interval	W+	W−	C
Slope (degree)	1	<5	−2.016	1.491	−3.507
	2	5–10	1.857	−0.446	2.303
	3	10–15	1.986	−0.319	2.305
	4	15–20	1.148	−0.091	1.239
	5	20–25	0.847	−0.037	0.883
	6	25–30	−1.557	0.012	−1.569
	7	30–35	0.000	0.009	−0.009
	8	35–40	0.000	0.004	−0.004
	9	40–45	0.000	0.001	−0.001
	10	>45	0.000	0.001	−0.001
Aspect (degree)	N	>22.5	0.227	−0.052	0.279
	NE	22.5–67.5	0.724	−0.152	0.876
	E	67.5–112.5	0.343	−0.018	0.360
	SE	112.5–157.5	−1.207	0.015	−1.223
	S	157.5–202.5	0.000	0.022	−0.022
	SW	202.5–247.5	0.000	0.033	−0.033
	W	247.5–292.5	0.043	−0.003	0.047
	NW	292.5–337.5	−0.080	0.029	−0.109
	N	337.5–360	−0.488	0.122	−0.610
Simplified lithological map	1	Bedrock	0.000	0.079	−0.079
	2	Sandy transgressive deposit	0.000	0.015	−0.015
	3	Sandy depositional terraces	1.161	−0.013	1.174
	4	Clayey slope	−0.226	0.011	−0.238
	5	Consolidated slope	0.921	−0.279	1.200
	6	Muddy shelf	−0.187	0.352	−0.540
Distance from river mouths (km)	1	<2	1.620	−0.091	1.711
	2	2–4	0.410	−0.157	0.566
	3	4–6	−0.582	0.182	−0.764
	4	6–8	−0.434	0.086	−0.520
	5	>8	0.042	−0.014	0.056
Distance from faults (km)	1	<1	0.975	−0.803	1.778
	2	1–2	0.234	−0.043	0.277
	3	2–3	−0.486	0.047	−0.532
	4	3–4	−1.168	0.093	−1.262
	5	>4	−1.982	0.416	−2.398

5.3. Susceptibility Map

The final susceptibility map has a continuous scale of numerical values, which need to be separated into susceptibility classes. The values of susceptibility were grouped into 5 classes (Very low, Low, Moderate, High, and Very High). The cut-off values of the susceptibility classes have set using Natural Breaks (i.e., a data classification method which identifies breakpoints where data values naturally cluster, creating categories that best represent the data distribution): Very Low: <0.05, Low: 0.05–0.20, Moderate: 0.20–0.40, High: 0.40–0.60, Very High: >0.60 (Figure 6a). Analyzing the results, the WoE method provided AUC values of 0.8922 for the test, 0.8873 for the training, and 0.8887 for the entire area (Figure 7). In general, these values mean that the models predicted approximately 88% of the instability events. The susceptibility map reveals that very low susceptibility is the most abundant susceptibility class (88% of the area, Figure 6a) and mainly corresponds to the continental shelf (Figure 4c). Low (4%), Moderate (4%), High (3%), and Very High (1%) susceptibility areas are principally located near the shelf edge or in upper slope sectors (Figure 6).

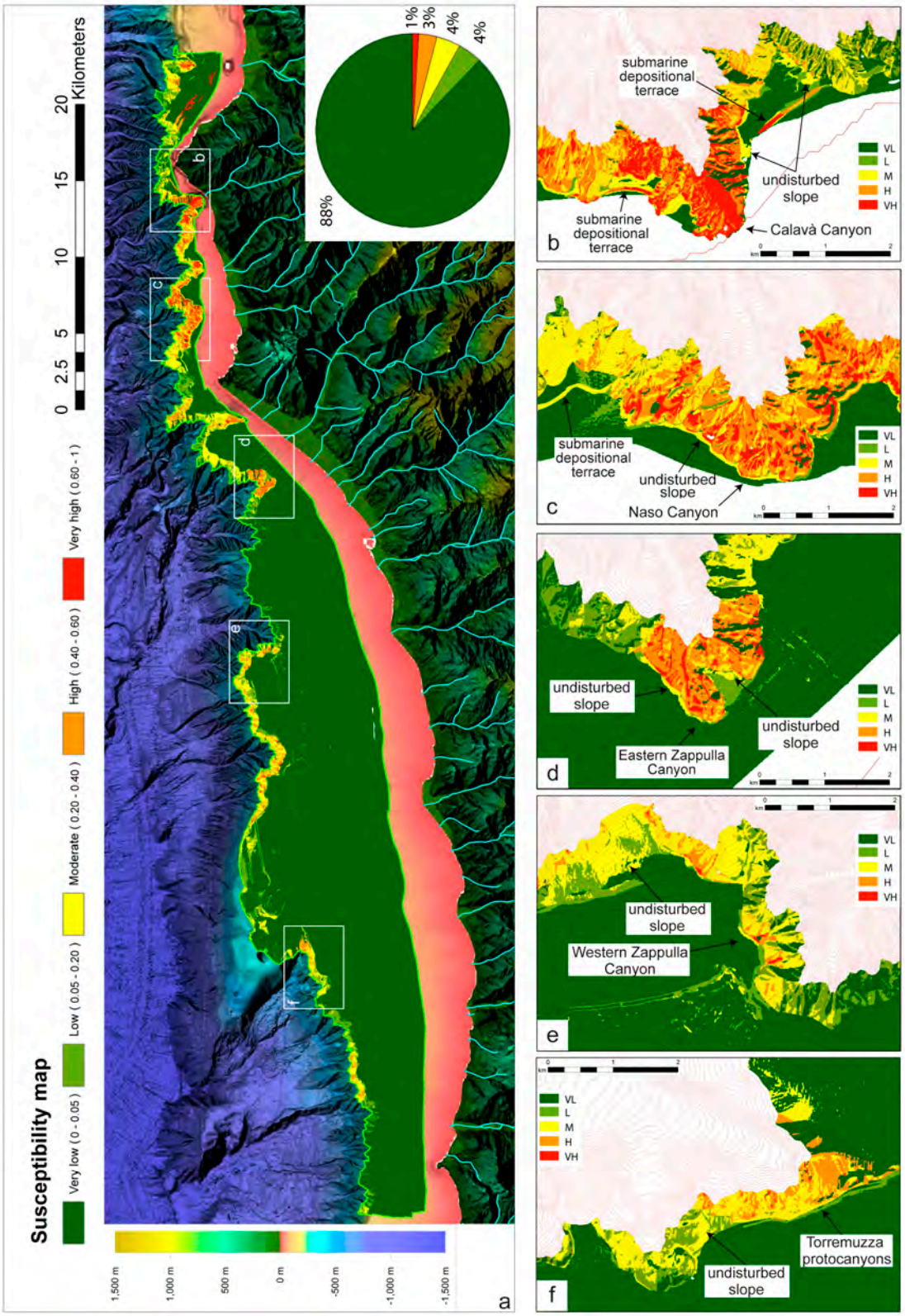

Figure 6. (**a**) Susceptibility map of the shallow-depth portion of the Capo d'Orlando continental margin, with a pie chart showing the percentage area of the different susceptibility classes. Insets (**b**–**f**) show zoomed-in views of selected areas of the map. The high resolution of the map allows for the identification, within individual canyon or slope segments, of areas with varying degrees of susceptibility. SDT stands for submarine depositional terrace. The contours are shown at 10 m intervals.

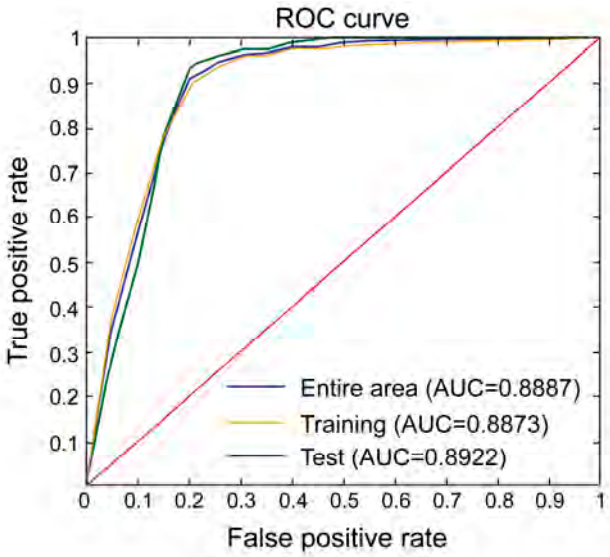

Figure 7. ROC curves and relative AUC of the test, training, and entire area.

6. Discussion

6.1. Preconditioning Factors Influence on Slope Destabilization

Slope stability is largely related to the combination of slope angle and material properties (friction angle, permeability, cohesion, shear, strain) [52]. The landslides of the study area negatively correlate with slope values <5° while strongly correlate with slope ranges of 5–15° and with consolidated formations outcrops (Figure 5).

According to areally limited lithologic information, the Noemi Unit, comprising hemipelagic clays and turbiditic deposits, outcrops in the canyons of the eastern portion of the study area [35]. Similar lithologies involved in subaerial landslides occur at slope ranges of 15–20° [61,62], which falls into the slope range obtained in this study. We interpret that the strong association between landslides and a slope range of 5–15° could be related to the lithology of the substrate. A submarine slope instability assessment performed in the Aveiro Canyon, western Portugal, found that slopes < 5° present low susceptibility to landslides, while slopes of 5–20° are highly susceptible to submarine landslides [63], matching the outcome of our study. The subsurface of the Aveiro district and its relative submarine portion, below the Quaternary unit, are characterized by marly clays, clayey, and subarkosic sandstones [64]. The similarity of the susceptible slope ranges in the study area and the Portuguese margin, both characterized by sedimentary soft rocks, could support the possible relation of the susceptible slope ranges with the lithology of the subsurface.

The strict relation between submarine landslides, slope values, and lithology is also highlighted by the positive correlation between shallow-water submarine landslides and sandy depositional terraces. Landslides often affect the surfaces of submarine depositional terraces, such as in the Aeolian archipelago [46,65] and Carini Embayment [66] in the Tyrrhenian Sea and Punta Alice canyon [67] in the Ionian Sea. Also, in the study area, a high percentage of landslides occur within the foresets of sandy depositional terraces despite their limited areal extension (Figures 4c and 5). We interpret that the high susceptibility to landslides involving the foresets of depositional terraces is principally due to their seaward steep slope, sufficient to destabilize poorly consolidated sediments. The primary role of slope angle in reducing slope stability is further supported by the lack of correlation between transgressive deposits and landslides. Transgressive deposits are mostly flat, being draped by Holocene deposition (Figure 4a); despite being characterized by a composition comparable with sandy depositional terraces, no significant correlation is observed between transgressive deposits and landslides (Figure 5).

In the study area, the contrast values highlighted a good correspondence between landslides and NE–E slope directions (Figure 5). The higher occurrence of landslides in slopes oriented toward NE and E is not biased by a major percentage of slope dipping towards those directions that, on the contrary, are less extended than the area dipping towards NW and W (Figure 4b). We have interpreted that longshore drift, flowing from W to E, could create thicker sand deposits on the western canyon side, eventually resulting in slope collapses directed towards the NE and E directions. Longshore currents transportation in the nearshore heads of submarine canyons is frequently reported in the literature [19,22,24,67–71]. Longshore current crossing canyon heads can lead to the asymmetric accumulation of sediments as reported in the Delgada Canyon, western North America, where grain-size analysis reported a higher percentage of sand and a coarser grain-size in the western side of the canyon head compared to the eastern one [70]. We interpret that in the study area, as in the Delgada Canyon, sediments are accumulated by longshore drift behind canyon heads located in narrow shelf portions becoming a preconditioning factor for shallow-depth landslides.

The distance from river mouths showed an increasing correlation with landslides as the distance decreased below 4 km. Landslide occurrence is also more probable at distances <2 km from rivers; this data is extremely significant considering that this class represents only 2% of the study area (Figure 4d). The analysis highlights 'distance to river mouths' as a novel preconditioning factor for submarine landslides. This factor appears to influence slope stability in areas where short, steep, and intermittent watersheds are near submarine canyons, a configuration commonly found along tectonically active continental margins [72]. The river distance map has been elaborated on the present-day river mouths, but during the last eustatic fall, which ended 18 ka, the river mouths in the northern Sicilian continental margin were closer to the actual shelf edge [45,73]. Pleistocene rivers discharged coarse-grained sediments on the shelf edge [73] developing, in some sectors of the northern Sicilian continental margin, progradational sedimentary wedges [74]. These wedges, perched along the shelf margin, have been locally involved in landsliding processes [74]. Rapid sedimentation can induce excess pore pressures in the sedimentary column and increase the shear strain, thereby contributing to slope destabilization [75]. Consequently, it must be considered that the impact of hyperpycnal flow generated at river mouths on the shelf edge decreased in time with the rise in the sea level. The timing of the submarine landslides in the study area is unknown; they potentially occurred between the last sea-level fall and the present day. Thus, the good correspondence between landslide susceptibility and the distance from river mouths could represent on one hand, the ancient contribution of sediment transportation and deposition operated by rivers once located near the shelf edge and, on the other, recent riverine processes testified by the presence of active submarine canyons fed by fluvial input (i.e., Calavà, Orlando and Eastern Zappulla canyons).

The correlation between distances from faults and landslides is particularly effective when they are at <1 km of distance (Figure 5). Slope instabilities are common in tectonically active areas characterized by high uplift rates where extensional faults dissect the sedimentary cover of the slope [76]. Local tectonic lineaments creating small steps in the slope as well as structural highs can influence canyons position [23,77–80]. Fault-generated scarps can influence the sediment routing, create oversteepened and overhanging portions susceptible to failure leading to canyon retrogression or enlargements [78,81]. The relation between faults and landslides can be unveiled through seismic sections or, when the surface of the scarps has not been extensively reworked, by high-resolution bathymetries. Nevertheless, if the action of erosive processes obliterates the fault scarp morphology, as in the

study area, our results show that the WoE method can, on a probabilistic level, determine the past influence of tectonic elements on slope stability.

6.2. From Landslide Susceptibility to Hazard Potential

The hazard (i.e., the likelihood of an event occurring within a specific timeframe and the potential intensity or magnitude of the event) related to submarine landslides is determined by their proximity to submarine infrastructures and landslides tsunamigenic potential. Tsunamis may be generated by submarine landslides when a complex coupling of landslide parameters occurs, such as landslide volume, motion, material properties, and water surface deformation [82].

The susceptibility analysis performed on the shallow-water portion of the Capo d'Orlando margin highlights that high to very high landslide susceptibility characterizes canyon heads and flanks (Figure 6b–f), submarine depositional terraces (Figure 6b,c) and moderate susceptibility characterize undisturbed portions of the slope landward from canyon heads (Figure 6b,d,e), where possible retrogressive landslides will be able to take place. Submarine landslide inventories highlight that small slides are more frequent on steep slopes (e.g., canyon heads and flanks) than on gentler slopes [15,48,83,84]. The steepness of the slope induces an intense disintegration of the failed mass, and the consequent water entrainment transforms landslides into debris flows and turbidity currents [1,10,13]. Disintegrative landslides occurring in canyons are more frequent but volumetrically small and with long runouts resulting in a low tsunamigenic potential. On the other hand, disintegrative landslides can be hazardous features for submarine infrastructures located on the seafloor (e.g., windfarms, submarine cables) or in shallow-water area regions where canyons are very close to the coast, as in the case of the Calavà, Naso, Eastern Zappulla Canyon, and Torremuzza protocanyons (Figure 6f).

Large and undisturbed portions of the slope are moderately susceptible to shallow-water landslides (Figure 6e). Landslides occurring on open slopes are potentially larger than those occurring at canyon heads and flanks since sediments can accumulate over large areas and for long time spans giving rise to large-scale failures [16,48]. Moreover, the permanence at the base of the headwall of part of the deposits suggests the cohesive behaviour of the failed mass [48]. Volumetrically large landslides composed of cohesive material are potentially more prone to generate high tsunami waves that could inundate coastlines, impact communities, global economies, and seafloor ecosystems.

The extrapolation of landslide magnitude, temporal frequency, and other parameters, particularly those regarding landslide motion (e.g., initial landslide acceleration), is needed for an accurate evaluation of the hazard potential. Moreover, quantifying landslide recurrence intervals, essential for probabilistic hazard models and for designing mitigation strategies, requires high-resolution stratigraphy of failure deposits. Nonetheless, susceptibility analysis represents the first step into the natural risk assessment offering the foundation for spatial vulnerability analysis; its integration with temporal and dynamic aspects of the landsliding process will contribute to assessing the overall risk of the study area.

6.3. Novelty and Criticalities

Submarine landslide susceptibility analyses are rare and mostly developed for open-slope landslides in deep-water environments. However, landslide scars are an almost ubiquitous feature at shelf edges, particularly in active margins carved by submarine canyons. This work represents the first attempt to quantify the most favourable conditions for generating shallow-water landslides, resulting in a detailed submarine landslide susceptibility map in a shallow-water sector of a continental margin. The described approach

is not time-consuming, as it is based on accessible preconditioning factors that can be easily extracted from existing national-scale datasets. Our approach resulted in a reliable model, indicating that it can also be applied in other shallow-water sectors characterized by limited databases representing a common scenario in the submarine environment. Moreover, the application of our approach to other study areas could provide more generalized insights into the key factors that predispose slope instability.

The main limitation of this work lies in the absence of direct measurements acquired in the study area. Some of the preconditioning factors used can be considered as proxies for geological processes that have not been directly measured (e.g., the distance from the river mouth is an exemplification of the impact of hyperpycnal flow). The simplified lithological map is based on morpho-bathymetric interpretation and bibliographic information. However, due to the lack of sampling data and homogeneous seismic sections, it is not possible to accurately estimate the sediment grain size distribution. Furthermore, in the case of "sandy transgressive deposits", "sandy depositional terraces", and "consolidated slope", it is not possible to determine the extent of their burial beneath Holocene sedimentation and thus to understand whether a landslide involves these lithologies or the overlying sedimentation.

Moreover, due to the absence of a homogeneous dataset, the analysis does not include a series of other possible preconditioning factors like earthquakes and fluid seeps.

The Italian earthquake catalogue covers earthquakes that occurred from the year 1000 onwards [85]. Nevertheless, since the landslides considered in this study potentially occurred between the last sea-level fall and the present day, using the location of recent earthquakes as a preconditioning factor would be misleading. Moreover, the absence of homogeneous seismic sections made it impossible to determine the possible presence of fluid seeps, as suggested by the occurrence of pockmarks, which have been excluded from the analysis despite their preconditioning potential. Nevertheless, the acquisition of geophysical data and sediment samples to better constrain the subsurface structure and calibrate the lithological interpretation could be easily integrated into the susceptibility analysis, resulting in an updated susceptibility map.

7. Conclusions

In this work, 450 landslide scars have been mapped and their combination, applying the Weight of Evidence method, with selected preconditioning factors, resulted in the submarine landslide susceptibility assessment of the shallow-water portion of the Capo d'Orlando continental margin. To strengthen our recognition of susceptible areas, in addition to the preconditioning factors commonly used in susceptibility analyses (i.e., slope, aspect, lithology, distance from faults), a new preconditioning factor specifically intended for the study area has been considered (i.e., distance from river mouths). From the contrast analysis, the most favourable conditions for predisposing landslides, in order of importance, are slopes with ranges between 5 and 15°; distance from faults <1 km; distance from river mouth <2 km; consolidated lithologies on the slope and sandy depositional terraces on the shelf; and slopes exposed toward NE and E. The comparison with Lapa et al. (2020) [63] pointed out that the occurrence of landslides in the study area at slope ranges of 5–15° could be related to the lithological composition of the slope comprising hemipelagic and turbiditic deposits. Our study represents one of the few susceptibility analyses performed in submarine canyons. More studies of this kind, in different geological contexts and where more strict lithological data are available, could provide important information about the critical slope angle of submarine landslides associated with different lithologies.

The increase in susceptibility with decreasing distance from river mouths indicates that river-related processes are an important preconditioning factor, eventually associated

with sediment accumulation operated by rivers. Also, longshore currents are identified as a shallow-water landslide preconditioning factor. Littoral currents, flowing from W to E, are interpreted to impact the slope stability due to the asymmetrical distribution of sediment around canyon heads, i.e., higher in the western portion coinciding with the destabilization of slopes exposed toward NE–E. Landslide susceptibility map in the Capo d'Orlando continental margin highlights that a very low susceptibility characterizes the continental shelf, while the shelf edge and upper slope portions present from low to very high susceptibility. Very high to moderate susceptible areas match regions where landslides have already occurred, such as in canyon heads and canyon flanks, but also in undisturbed portions on the slope and landward from canyon heads, highlighting the potential for retrogressive landslides. In conclusion, our results are promising and show that this approach can be applied to obtain a preliminary susceptibility assessment in areas with a limited database. Moreover, this approach may be useful for the selection of specific areas to be studied in more detail through site investigations required to support physically based slope stability analysis.

Author Contributions: Conceptualization, E.S., D.C. and F.L.C.; methodology, E.S.; software, E.S.; validation, E.S.; formal analysis, E.S.; investigation, E.S.; resources, F.G. and F.L.C.; data curation, E.S.; writing—original draft preparation, E.S.; writing—review and editing, E.S., D.C., F.G., D.S., M.B. and F.L.C.; visualization, E.S.; supervision, D.C., F.G., D.S. and F.L.C.; project administration, F.L.C.; funding acquisition, F.L.C. All authors have read and agreed to the published version of the manuscript.

Funding: The study was carried out within the RETURN Extended Partnership and received funding from the European Union's Next Generation EU package (National Recovery and Resilience Plan—NRRP, Mission 4, Component 2, Investment 1.3—D.D. 1243 2/8/2022, PE0000005).

Data Availability Statement: The raw data supporting the conclusions of this article will be made available by the authors on request.

Acknowledgments: The authors wish to thank the anonymous reviewers for their suggestions, which helped improve the quality of the work. Special thanks go to Alessandra Mercorella, Andrea Gallerani, Fabio Savelli, and Elisa Leidi for their contributions to data processing and management. We also gratefully acknowledge Matteo Berti for his support in the use of the graphical user interface, and Carlo Esposito and Chiara Martinello for the valuable discussions on susceptibility-related aspects. Finally, the authors acknowledge the project referred to in the funding section.

Conflicts of Interest: The authors declare no conflicts of interest. The funders had no role in the design of the study, in the collection, analyses, or interpretation of data, in the writing of the manuscript, or in the decision to publish the results.

Abbreviations

The following abbreviations are used in this manuscript:

WoE	Weight of Evidence
LIP	Landslide Initiation Point
ROC	Receiver Operating Characteristic
AUC	Area under the Curve

References

1. Masson, D.G.; Harbitz, C.B.; Wynn, R.B.; Pedersen, G.; Løvholt, F. Submarine Landslides: Processes, Triggers and Hazard Prediction. *Philos. Trans. R. Soc. A Math. Phys. Eng. Sci.* **2006**, *364*, 2009–2039. [CrossRef] [PubMed]
2. Camerlenghi, A.; Urgeles, R.; Ercilla, G.; Brückmann, W. Scientific Ocean Drilling behind the Assessment of Geo-Hazards from Submarine Slides. *Sci. Drill.* **2007**, *4*, 45–47. [CrossRef]

3. Talling, P.J.; Clare, M.; Urlaub, M.; Pope, E.; Hunt, J.E.; Watt, S.F.L. Large Submarine Landslides on Continental Slopes: Geohazards, Methane Release, and Climate Change. *Oceanography* **2014**, *27*, 32–45. [CrossRef]
4. Chiocci, F.L.; Casalbore, D.; Falese, F.; Spatola, D.; Scacchia, E.; Bianchini, M. Marine Geohazards in Italy, Their Specificity and Mitigation Perspective. In *Marine Hazards, Coastal Vulnerability, Risk (mis)Perceptions—A Mediterranean Perspective*; CIESM Monographs 52; Briand, F., Ed.; CIESM Publisher: Paris, France; Monaco, France, 2024; pp. 73–88.
5. Dan, G.; Sultan, N.; Savoye, B. The 1979 Nice Harbour Catastrophe Revisited: Trigger Mechanism Inferred from Geotechnical Measurements and Numerical Modelling. *Mar. Geol.* **2007**, *245*, 40–64. [CrossRef]
6. Zaniboni, F.; Armigliato, A.; Pagnoni, G.; Tinti, S. Continental Margins as a Source of Tsunami Hazard: The 1977 Gioia Tauro (Italy) Landslide-Tsunami Investigated through Numerical Modeling. *Mar. Geol.* **2014**, *357*, 210–217. [CrossRef]
7. Hughes Clarke, J.E.; Shor, A.N.; Piper, D.J.; Mayer, L.A. Large-scale Current-induced Erosion and Deposition in the Path of the 1929 Grand Banks Turbidity Current. *Sedimentology* **1990**, *37*, 613–629. [CrossRef]
8. Pope, E.L.; Talling, P.J.; Carter, L. Which Earthquakes Trigger Damaging Submarine Mass Movements: Insights from a Global Record of Submarine Cable Breaks? *Mar. Geol.* **2017**, *384*, 131–146. [CrossRef]
9. Colantoni, P.; Gennesseaux, M.; Vanney, J.R.; Ulzega, A.; Trombetta, A. Processi Dinamici Del Canyon Sottomarino de Gioia Tauro (Mare Tirreno). *G. Geol. Ser. 3* **1992**, *54*, 199–213.
10. Mulder, T.; Cochonat, P. Classification of Offshore Mass Movements. *J. Sediment. Res.* **1996**, *66*, 43–57. [CrossRef]
11. Locat, J.; Lee, H.J. Submarine Landslides: Advances and Challenges. *Can. Geotech. J.* **2002**, *39*, 193–212. [CrossRef]
12. Lee, H.J.; Locat, J.; Desgagnés, P.; Parsons, J.D.; McAdoo, B.G.; Orange, D.L.; Puig, P.; Wong, F.L.; Dartnell, P.; Boulanger, E. Submarine Mass Movements on Continental Margins. In *Continental Margin Sedimentation: From Sediment Transport to Sequence Stratigraphy*; Wiley: New York, NY, USA, 2007; pp. 213–274. [CrossRef]
13. Huhn, K.; Arroyo, M.; Cattaneo, A.; Clare, M.A.; Gràcia, E.; Harbitz, C.B.; Krastel, S.; Kopf, A.; Løvholt, F.; Rovere, M.; et al. *Part II Submarine Landslide Deposits in Current Active and Passive Margins*; John Wiley & Sons, Inc.: New York, NY, USA, 2019.
14. Chaytor, J.D.; ten Brink, U.S.; Solow, A.R.; Andrews, B.D. Size Distribution of Submarine Landslides along the U.S. Atlantic Margin. *Mar. Geol.* **2009**, *264*, 16–27. [CrossRef]
15. Casas, D.; Chiocci, F.; Casalbore, D.; Ercilla, G.; de Urbina, J.O. Magnitude-Frequency Distribution of Submarine Landslides in the Gioia Basin (Southern Tyrrhenian Sea). *Geo-Marine Lett.* **2016**, *36*, 405–414. [CrossRef]
16. Casalbore, D.; Bosman, A.; Casas, D.; Chiocci, F.; Martorelli, E.; Ridente, D. Morphological Variability of Submarine Mass Movements in the Tectonically–Controlled Calabro–Tyrrhenian Continental Margin (Southern Italy). *Geosciences* **2019**, *9*, 43. [CrossRef]
17. Urlaub, M.; Talling, P.J.; Masson, D.G. Timing and Frequency of Large Submarine Landslides: Implications for Understanding Triggers and Future Geohazard. *Quat. Sci. Rev.* **2013**, *72*, 63–82. [CrossRef]
18. Kelner, M.; Migeon, S.; Tric, E.; Couboulex, F.; Dano, A.; Lebourg, T.; Taboada, A. Frequency and Triggering of Small-Scale Submarine Landslides on Decadal Timescales: Analysis of 4D Bathymetric Data from the Continental Slope Offshore Nice (France). *Mar. Geol.* **2016**, *379*, 281–297. [CrossRef]
19. Biscara, L.; Hanquiez, V.; Leynaud, D.; Marieu, V.; Mulder, T.; Gallissaires, J.M.; Crespin, J.P.; Braccini, E.; Garlan, T. Submarine Slide Initiation and Evolution Offshore Pointe Odden, Gabon—Analysis from Annual Bathymetric Data (2004–2009). *Mar. Geol.* **2012**, *299–302*, 43–50. [CrossRef]
20. Pratson, L.F.; Coakley, B.J. A Model for the Headward Erosion of Submarine Canyons Induced by Downslope-Eroding Sediment Flows. *Bull. Geol. Soc. Am.* **1996**, *108*, 225–234. [CrossRef]
21. Micallef, A.; Mountjoy, J.J.; Canals, M.; Lastras, G. Deep-Seated Bedrock Landslides and Submarine Canyon Evolution in an Active Tectonic Margin: Cook Strait, New Zealand. In *Submarine Mass Movements and Their Consequences. Advances in Natural and Technological Hazards Research*; Springer: Berlin/Heidelberg, Germany, 2012; pp. 201–212. [CrossRef]
22. Harishidayat, D.; Niyazi, Y.; Stewart, H.A.; Al-Shuhail, A.; Jamieson, A.J. Submarine Canyon Development Controlled by Slope Failure and Oceanographic Process Interactions. *Sci. Rep.* **2024**, *14*, 18486. [CrossRef] [PubMed]
23. Shepard, F.P. Submarine Canyons: Multiple Causes and Long-Time Persistence. *Am. Assoc. Pet. Geol. Bull.* **1981**, *65*, 1062–1077. [CrossRef]
24. Gamberi, F.; Rovere, M.; Marani, M.P.; Dykstra, M. Modern Submarine Canyon Feeder-System and Deep-Sea Fan Growth in a Tectonically Active Margin (Northern Sicily). *Geosphere* **2015**, *11*, 307–319. [CrossRef]
25. Avdievitch, N.N.; Coe, J.A. Submarine Landslide Susceptibility Mapping in Recently Deglaciated Terrain, Glacier Bay, Alaska. *Front. Earth Sci.* **2022**, *10*, 821188. [CrossRef]
26. Borrell, N.; Somoza, L.; León, R.; Medialdea, T.; Gonzalez, F.J.; Gimenez-Moreno, C.J. GIS Catalogue of Submarine Landslides in the Spanish Continental Shelf: Potential and Difficulties for Susceptibility Assessment. *Adv. Nat. Technol. Hazards Res.* **2016**, *41*, 499–508. [CrossRef]
27. León, R.; Somoza, L. GIS-Based Mapping for Marine Geohazards in Seabed Fluid Leakage Areas (Gulf of Cadiz, Spain). *Mar. Geophys. Res.* **2011**, *32*, 207–223. [CrossRef]

28. Tarazona, D.M.; Prieto, J.; Murphy, W.; Vesga, J.N.; Rincon, D.; Munoz, C.H.; Pinzon, H.M.; Mora, A.M.; Acuña-Uribe, M. Submarine Landslide Susceptibility Assessment along the Southern Convergent Margin of the Colombian Caribbean. *Lead. Edge* **2023**, *42*, 344–359. [CrossRef]
29. Glade, T.; Crozier, M.J. The Nature of Landslide Hazard Impact. In *Landslide Hazard Risk*; Wiley: New York, NY, USA, 2005; pp. 41–74.
30. Catalano, R.; Lo Cicero, G.; Sulli, A. Geology of Sicily: An Introduction. General Field Trip Guide. In Proceedings of the VI International Symposium on the Jurassic System, Palermo, Italy, 12–22 September 2002; pp. 12–22. Available online: https://www.pemberleybooks.com/product/geology-of-sicily-an-introduction.-general-field-trip-guide-vi-international-symposium-on-the-jurassic-system-palermo-italy-12-22-september-2002/26038/ (accessed on 13 July 2025).
31. Kastens, K.A.; Mascle, J. The Geological Evolution of the Tyrrhenian Sea: An Introduction to the Scientific Results of ODP Leg 107. In *Proceedings of the Ocean Drilling Program, 107 Scientific Results*; Ocean Drilling Program: College Station, TX, USA, 1990; pp. 3–26. [CrossRef]
32. Pepe, F.; Bertotti, G.; Cella, F.; Marsella, E. Rifted Margin Formation in the South Tyrrhenian Sea: A High-Resolution Seismic Profile across the North Sicily Passive Continental Margin. *Tectonics* **2000**, *19*, 241–257. [CrossRef]
33. Pepe, F.; Sulli, A.; Agate, M.; Di Maio, D.; Kok, A.; Lo Iacono, C.; Catalano, R. Plio-Pleistocene Geological Evolution of the Northern Sicily Continental Margin (Southern Tyrrhenian Sea): New Insights from High-Resolution, Multi-Electrode Sparker Profiles. *Geo-Marine Lett.* **2003**, *23*, 53–63. [CrossRef]
34. Milia, A.; Iannace, P.; Tesauro, M.; Torrente, M.M. Marsili and Cefalù Basins: The Evolution of a Rift System in the Southern Tyrrhenian Sea (Central Mediterranean). *Glob. Planet. Change* **2018**, *171*, 225–237. [CrossRef]
35. Catalano, R.; Di Maio, D.; Sulli, A.; Analfino, A. *Carta Geologica d'Italia Alla Scala 1:50.000 Del Foglio 599 "Patti (Settore Marino)"*; ISPRA, Servizio Geologico d'Italia: Rome, Italy, 2013.
36. Nigro, F.; Sulli, A. Plio-Pleistocene Extensional Tectonics in the Western Peloritani Area and Its Offshore (Northeastern Sicily). *Tectonophysics* **1995**, *252*, 295–305. [CrossRef]
37. Billi, A.; Presti, D.; Orecchio, B.; Faccenna, C.; Neri, G. Incipient Extension along the Active Convergent Margin of Nubia in Sicily, Italy: Cefal-Etna Seismic Zone. *Tectonics* **2010**, *29*, 1–20. [CrossRef]
38. Antonioli, F.; Ferranti, L.; Fontana, A.; Amorosi, A.; Bondesan, A.; Braitenberg, C.; Dutton, A.; Fontolan, G.; Furlani, S.; Lambeck, K.; et al. Holocene Relative Sea-Level Changes and Vertical Movements along the Italian and Istrian Coastlines. *Quat. Int.* **2009**, *206*, 102–133. [CrossRef]
39. Ferranti, L.; Antonioli, F.; Mauz, B.; Amorosi, A.; Dai Pra, G.; Mastronuzzi, G.; Monaco, C.; Orrù, P.; Pappalardo, M.; Radtke, U.; et al. Markers of the Last Interglacial Sea-Level High Stand along the Coast of Italy: Tectonic Implications. *Quat. Int.* **2006**, *145–146*, 30–54. [CrossRef]
40. Sulli, A.; Lo Presti, V.; Gasparo Morticelli, M.; Antonioli, F. Vertical Movements in NE Sicily and Its Offshore: Outcome of Tectonic Uplift during the Last 125 Ky. *Quat. Int.* **2013**, *288*, 168–182. [CrossRef]
41. Menna, M.; Poulain, P.M.; Ciani, D.; Doglioli, A.; Notarstefano, G.; Gerin, R.; Rio, M.H.; Santoleri, R.; Gauci, A.; Drago, A. New Insights of the Sicily Channel and Southern Tyrrhenian Sea Variability. *Water* **2019**, *11*, 1355. [CrossRef]
42. Spatola, D.; Sulli, A.; Casalbore, D.; Chiocci, F.L. First Evidence of Contourite Drifts in the North-Western Sicilian Active Continental Margin (Southern Tyrrhenian Sea). *J. Mar. Sci. Eng.* **2021**, *9*, 1043. [CrossRef]
43. Marina, I.I. *Della Atlante Della Correnti Superficiali Dei Mari Italiani*; Istituto Idrografico della Marina: Genova, Italy, 1982.
44. Lo Presti, V.; Antonioli, F.; Casalbore, D.; Chiocci, F.L.; Lanza, S.; Sulli, A.; Randazzo, G. Geohazard Assessment of the North-Eastern Sicily Continental Margin (SW Mediterranean): Coastal Erosion, Sea-Level Rise and Retrogressive Canyon Head Dynamics. *Mar. Geophys. Res.* **2022**, *43*, 1134385. [CrossRef]
45. Gamberi, F. Systems Supplying Sediment to Canyon Heads (SSSCHs) in the Tyrrhenian Sea: The Past and the Present as a Key to Understanding Deep-Sea Stratigraphy. *Mar. Pet. Geol.* **2020**, *119*, 104470. [CrossRef]
46. Casalbore, D.; Falese, F.; Martorelli, E.; Romagnoli, C.; Chiocci, F.L. Submarine Depositional Terraces in the Tyrrhenian Sea as a Proxy for Paleo-Sea Level Reconstruction: Problems and Perspective. *Quat. Int.* **2017**, *439 Pt A*, 169–180. [CrossRef]
47. Gamberi, F.; Casalbore, D.; Marani, M.; Rovere, M.; Bosman, A.; Calarco, M.; Dalla Valle, G.; Leidi, E.; Martorelli, E.; Mercorella, A.; et al. Geohazard Features of the Aeolian Island Slopes and the North-Eastern Sicily Offshore. *J. Maps* **2024**, *20*, 2343314. [CrossRef]
48. Casalbore, D.; Martorelli, E.; Bosman, A.; Morelli, E.; Chiocci, F.L. Failure Dynamics of Landslide Scars on the Lower Continental Slope of the Tyrrhenian Calabrian Margin: Insights from an Integrated Morpho-Bathymetric and Seismic Analysis. *Geol. Soc. Spec. Publ.* **2019**, *477*, 389–397. [CrossRef]
49. Lombardo, L.; Cama, M.; Maerker, M.; Rotigliano, E. A Test of Transferability for Landslides Susceptibility Models under Extreme Climatic Events: Application to the Messina 2009 Disaster. *Nat. Hazards* **2014**, *74*, 1951–1989. [CrossRef]

50. Esposito, C.; Mastrantoni, G.; Marmoni, G.M.; Antonielli, B.; Caprari, P.; Pica, A.; Schilirò, L.; Mazzanti, P.; Bozzano, F. From Theory to Practice: Optimisation of Available Information for Landslide Hazard Assessment in Rome Relying on Official, Fragmented Data Sources. *Landslides* **2023**, *20*, 2055–2073. [CrossRef]
51. Martinello, C.; Delchiaro, M.; Iacobucci, G.; Cappadonia, C.; Rotigliano, E.; Piacentini, D. Exploring the Geomorphological Adequacy of the Landslide Susceptibility Maps: A Test for Different Types of Landslides in the Bidente River Basin (Northern Italy). *Catena* **2024**, *238*, 107835. [CrossRef]
52. Çellek, S. Effect of the Slope Angle and Its Classification on Landslides. *Himal. Geol.* **2022**, *43*, 85–95.
53. Yuvaraj, R.M.; Dolui, B. Geographical Assessment of Landslide Susceptibility Using Statistical Approach. *Quat. Sci. Adv.* **2023**, *11*, 100097. [CrossRef]
54. Çellek, S. The Effect of Aspect on Landslide and Its Relationship with Other Parameters. In *Landslides*; IntechOpen: Rijeka, Croatia, 2022; p. 13.
55. Casalbore, D.; Chiocci, F.L.; Mugnozza, G.S.; Tommasi, P.; Sposato, A. Flash-Flood Hyperpycnal Flows Generating Shallow-Water Landslides at Fiumara Mouths in Western Messina Strait (Italy). *Mar. Geophys. Res.* **2011**, *32*, 257–271. [CrossRef]
56. METIQ Working Group Quaternary Map of Italy, Scale 1:500,000, 5 Sheets. Ed. by ISPRA, Draft Version Ed. INQUA Congr. Roma. 2023. Available online: https://sgi.isprambiente.it/metiq/METIQ_Explanatory_Note.pdf (accessed on 13 July 2025).
57. Gamberi, F.; Scacchia, E.; Ferrante, V. Submarine Landslides, Debris Flows and Canyons: Processes of Slope Degradation and Shelf-Edge Indentation in a Tectonically Active Margin (Finale Basin, Northern Sicilian Margin, Tyrrhenian Sea). *Front. Earth Sci.* 2025, *submitted*.
58. Bonham-Carter, G.F. Weights of Evidence Modelling: A New Approach to Mapping Mineral Potential. In *Statistical Applications in the Earth Sciences*; Geological Survey of Canada: Ottawa, ON, Canada, 1989; pp. 171–183.
59. Sadisun, I.A.; Telaumbanua, J.A.; Kartiko, R.D.; Dinata, I.A. Pamela Weight of Evidence Method for Landslide Susceptibility Mapping in Sigi Biromaru, Central Sulawesi. *IOP Conf. Ser. Earth Environ. Sci.* **2021**, *830*, 7–13. [CrossRef]
60. Bhandari, B.P.; Dhakal, S.; Tsou, C.Y. Assessing the Prediction Accuracy of Frequency Ratio, Weight of Evidence, Shannon Entropy, and Information Value Methods for Landslide Susceptibility in the Siwalik Hills of Nepal. *Sustainability* **2024**, *16*, 2092. [CrossRef]
61. Berti, M.; Bertello, L.; Bernardi, A.R.; Caputo, G. Back Analysis of a Large Landslide in a Flysch Rock Mass. *Landslides* **2017**, *14*, 2041–2058. [CrossRef]
62. Squarzoni, G.; Bayer, B.; Franceschini, S.; Simoni, A. Pre- and Post-Failure Dynamics of Landslides in the Northern Apennines Revealed by Space-Borne Synthetic Aperture Radar Interferometry (InSAR). *Geomorphology* **2020**, *369*, 107353. [CrossRef]
63. Lapa, N.; Marques, F.M.F.S.; Rodrigues, A. Aveiro Canyon Head (Portugal) Submarine Slope Instability Assessment. *Appl. Sci.* **2020**, *10*, 9038. [CrossRef]
64. De Melo, M.C.; Paquete, P.C.; Da Silva, M.M. Evolution of the Aveiro Cretaceous Aquifer (NW Portugal) During the Late Pleistocene and Present Day: Evidence from Chemical and Isotopic Data. In *Palaeowaters in Coastal Europe: Evolution of Groundwater Since the Late Pleistocene*; Special Publications; Edmunds, W.M., Milne, C.J., Eds.; Geological Society of London: London, UK, 2001; p. 189.
65. Casalbore, D.; Romagnoli, C.; Adami, C.; Bosman, A.; Falese, F.; Ricchi, A.; Chiocci, F.L. Submarine Depositional Terraces at Salina Island (Southern Tyrrhenian Sea) and Implications on the Late-Quaternary Evolution of the Insular Shelf. *Geoscience* **2018**, *8*, 20. [CrossRef]
66. Agate, M.; Infuso, S.; Lucido, M.; Mancuso, M. Submerged Depositional Terraces off the Carini Embayment (Northwestern Sicily). In *Atlante dei Terrazzi Deposizionali Sommersi Lungo le Coste Italiane*; Memorie Descrittive della Carta Geologica d'Italia; Chiocci, F.L., D'Angelo, S., Romagnoli, C., Eds.; Italian Institute for Environmental Protection and Research: Rome, Italy, 2004; Volume 58, pp. 66–68.
67. Casalbore, D.; Bosman, A.; Chiocci, F.L. Study of Recent Small-Scale Landslides in Geologically Active Marine Areas Through Repeated Multibeam Surveys: Examples from the Southern Italy. In *Submarine Mass Movements and Their Consequences. Advances in Natural and Technological Hazards Research*; Springer: Berlin/Heidelberg, Germany, 2012; pp. 573–582. [CrossRef]
68. Normark, W.R.; Piper, D.J.W.; Romans, B.W.; Covault, J.A.; Dartnell, P.; Sliter, R.W. Submarine Canyon and Fan Systems of the California Continental Borderland. *Spec. Pap. Geol. Soc. Am.* **2009**, *454*, 141–168. [CrossRef]
69. Yoshikawa, S.; Nemoto, K. Seasonal Variations of Sediment Transport to a Canyon and Coastal Erosion along the Shimizu Coast, Suruga Bay, Japan. *Mar. Geol.* **2010**, *271*, 165–176. [CrossRef]
70. Smith, M.E.; Werner, S.H.; Buscombe, D.; Finnegan, N.J.; Sumner, E.J.; Mueller, E.R. Seeking the Shore: Evidence for Active Submarine Canyon Head Incision Due to Coarse Sediment Supply and Focusing of Wave Energy. *Geophys. Res. Lett.* **2018**, *45*, 12403–12413. [CrossRef]
71. Joerger, S.T.; Smith, M.E.; Buscombe, D.; Mueller, E.R. Evidence for Littoral Convergence and Sediment Delivery to Mattole Submarine Canyon, Northern California. *Front. Earth Sci.* **2024**, *12*, 1377997. [CrossRef]
72. Bührig, L.H.; Colombera, L.; Patacci, M.; Mountney, N.P.; McCaffrey, W.D. Tectonic Influence on the Geomorphology of Submarine Canyons: Implications for Deep-Water Sedimentary Systems. *Front. Earth Sci.* **2022**, *10*, 836823. [CrossRef]

73. Caruso, A.; Cosentino, C.; Pierre, C.; Sulli, A. Sea-Level Changes during the Last 41,000 Years in the Outer Shelf of the Southern Tyrrhenian Sea: Evidence from Benthic Foraminifera and Seismostratigraphic Analysis. *Quat. Int.* **2011**, *232*, 122–131. [CrossRef]
74. Sulli, A.; Agate, M.; Mancuso, M.; Pepe, F.; Pennino, V.; Polizzi, S.; Presti, V.L.; Gargano, F.; Interbartolo, F. Variability of Depositional Setting along the North-Western Sicily Continental Shelf (Italy) during Late Quaternary: Effects of Sea Level Changes and Tectonic Evolution. *Alp. Mediterr. Quat.* **2012**, *25*, 141–155.
75. Kou, H.; Wang, Y.; Lu, J.; Yang, Y. Landslide Mechanism under Rapid Sedimentation in Shelf-Slope Break. *Appl. Ocean Res.* **2024**, *153*, 104242. [CrossRef]
76. Kanamatsu, T.; Ashi, J.; Shiraishi, K. Controlling Factors of a Submarine Landslide on the Kumano-Nada Continental Slope, West Japan. *Tectonophysics* **2024**, *883*, 230370. [CrossRef]
77. Ediger, V.; Okyar, M.; Ergin, M. Seismic Stratigraphy of the Fault-Controlled Submarine Canyon/Valley System on the Shelf and Upper Slope of Anamur Bay, Northeastern Mediterranean Sea. *Mar. Geol.* **1993**, *115*, 129–142. [CrossRef]
78. Mountjoy, J.J.; Barnes, P.M.; Pettinga, J.R. Morphostructure and Evolution of Submarine Canyons across an Active Margin: Cook Strait Sector of the Hikurangi Margin, New Zealand. *Mar. Geol.* **2009**, *260*, 45–68. [CrossRef]
79. Morelli, E.; Martorelli, E.; Casalbore, D.; Chiocci, F.L. Morpho-Stratigraphic Evolution of a Tectonically Controlled Canyon-Channel System in the Gioia Basin (Southern Tyrrhenian Sea). *Mar. Geol.* **2022**, *451*, 106881. [CrossRef]
80. Jin, L.; Luan, X.; Raveendrasinghe, T.D.; Jiang, L.; Xue, Y.; Wei, X.; Ma, H. Influence of Sedimentary Processes and Fault Tectonics on the Evolution of Submarine Canyons in the East Andaman Basin: Insights from High-Resolution Seismic Data Analysis. *Geomorphology* **2024**, *254*, 109179. [CrossRef]
81. Cabrera, C.; Puig, P.; Durán, R.; Fabri, M.C.; Guerin, C.; Lo Iacono, C.; Huvenne, V.A.I. Geomorphology and Evolution of the Blanes Canyon (NW Mediterranean). New Insights from High Resolution Mapping of Vertical Cliffs. *Geomorphology* **2024**, *461*, 109290. [CrossRef]
82. Roger, J.H.; Bull, S.; Watson, S.J.; Mueller, C.; Hillman, J.I.; Wolter, A.; Davidson, S.A. A Review of Approaches for Submarine Landslide-Tsunami Hazard Identification and Assessment. *Mar. Pet. Geol.* **2024**, *162*, 106729. [CrossRef]
83. McAdoo, B.G.; Pratson, L.F.; Orange, D.L. Submarine Landslide Geomorphology, US Continental Slope. *Mar. Geol.* **2000**, *169*, 103–136. [CrossRef]
84. Hühnerbach, V.; Masson, D.G. Landslides in the North Atlantic and Its Adjacent Seas: An Analysis of Their Morphology, Setting and Behaviour. *Mar. Geol.* **2004**, *213*, 343–362. [CrossRef]
85. Rovida, A.; Locati, M.; Camassi, R.; Lolli, B.; Gasperini, P. The Italian Earthquake Catalogue CPTI15. *Bull. Earthq. Eng.* **2020**, *18*, 2953–2984. [CrossRef]